Int. J. Electrochem. Sci., 15 **(2020)** 10684 – 10693, doi: 10.20964/2020.11.68

International Journal of
ELECTROCHEMICAL
SCIENCE
www.electrochemsci.org

Synthesis of Mesoporous Bi_2WO_6 Flower-Like Spheres with Photocatalysis Properties under Visible Light

Zhenqiong Gou[*], *Jinhang Dai, Jinwu Bai*[*],

College of Environment and Resources, Chongqing Technology and Business University, Chongqing 400067, P.R. China.
[*]E-mail: dorisgzq@163.com

Received: 5 August 2020 / *Accepted:* 14 September 2020 / *Published:* 30 September 2020

3D mesoporous Bi_2WO_6 flower-like spheres, which compose of nanosheets, were successfully synthesized by simple hydrothermal treatment. Bi_2WO_6 flower-like spheres exhibited high photocatalytic activity to tetracycline under visible light irradiation, because of the mesoporous structure, narrowed band gap and high surface area. Therefore, 3D mesoporous Bi_2WO_6 flower-like spheres can be a promising candidate material to be applied to the field of wastewater treatment.

Keywords: Bi_2WO_6; photocatalysis; visible light; tetracycline.

1. INTRODUCTION

Bi_2WO_6, has a layered structure, with the perovskite-like $[WO_4]^{2-}$ layers sandwiched between bismuth oxide $[Bi_2O_2]^{2+}$ ones [1-3]. Bi_2WO_6 is identified as an excellent photocatalyst due to the non-toxicity, strong oxidizing power, inexpensiveness, suitable energy band corresponding to the visible and ultraviolet light absorption with wave length less than 450 nm [4]. As it is well-known that the photocatalytic performance of the material is strongly associated with the morphology, the crystal structure, surface area, and crystal size [5,6]. Therefore, the controlling on morphology of the material can lead to the unique properties and promising application has aroused great interest. Until now, intensive researches have been focused on controlling the various morphologies of Bi_2WO_6 to enhance its photocatalytic activity. Among different morphologies of Bi_2WO_6, three-dimensional (3D) mesoporous structures have attracted much attention because the 3D mesoporous structures possess a large surface area, which provides more active sites and benefits the contact of photocatalyst with organic contaminants. Meanwhile, the mesoporous structure endows the photocatalyst with high absorption property and then enhance the photocatalytic performance of photocatalyst further [7].

Tetracycline (TC) plays a very important role in modern life, and it has been widely applied in medicine and stock breeding, but the large-scale abuse of TC has led to serious environmental problems,

contaminating water in lakes in particular. However, it is reported that more than 50% of drinking water comes from lakes. It is obvious and urgent that contamination caused by TC should be tackled by taking effective measures.

Herein, we successfully synthesized 3D Bi_2WO_6 flower-like spheres composing of 2D nanosheets through simple hydrothermal treatment. When exposed to visible light, Bi_2WO_6 flower-like spheres exhibited high photodegradation performance to TC, which can be explained by its feature that it possesses mesoporous structure, high crystallinity, narrowed band gap and high surface area.

2. EXPERIMENTAL SECTION

2.1 Preparation of Bi_2WO_6 flower-like spheres.

In a typical synthesis, 0.97 g $Bi(NO_3)_3 \cdot 5H_2O$ was dissolved in 10 mL glacial acetic acid solution, and subsequently, 0.33 g $Na_2WO_4 \cdot 2H_2O$ was added to the mixed solution, with absolute ethyl alcohol and distilled water (the volume ratio is 1:1) added. After stirring 30 min, the mixture was transferred into a 50 mL Teflon-lined autoclave and maintained at 180 °C for 24 h. The resulting precipitates was collected and washed with deionized water and absolute ethanol thoroughly and dried at 80 °C.

2.2 Characterizations

The X-ray diffractometer (XRD) diffractograms of samples were obtained using a diffractometer (Rigaka D/max2500) of Cu Kα radiation (λ = 1.540 56 A).

The surface morphologies of samples were scanned by a JEOLJSM-6700F scanning electron microscope (SEM) and a JEOL-2010, with an operating voltage of 200 kV transmission electron microscopy (TEM) .

The property of samples were characterized by ultraviolet-visible spectroscopy (UV-vis) diffuse reflectance spectra (DRS).

The Tristar 3000 nitrogen adsorption equipment was used to measure the Brunauer-Emmett-Teller (BET) specific surface areas and corresponding to pore-size distribution of as-prepared samples.

The ultra performance liquid chromatography (UPLC)-mass spectrum (MS) apparatus (ACQUITY UPLC I-CLASS/Xevo TQ-S) was utilized to investigate the mediate products of photodegradation TC.

2.3 Photodegradation experiments

An XPA-7 photochemical reactor from Nanjing Xujiang Electromechanical Plant (China) was applied to conduct photocatalytic degradation experiments. Experiments of the photodegradation generally followed our previous work,as reported in our previous literature [8], the photocatalytic reactions of the samples were evaluated by degradation of TC under 500 W Xe light. At room

temperature, 0.050 g samples well-prepared were added to 50 mL of a 15 mg/L TC aqueous solution. Before the illumination, the suspension was magnetically stirred in the dark for 30 min to make sure the establishment of an adsorption-desorption equilibrium between the TC and the photocatalyst. At the given intervals, approximately 5 mL of the sample solution were collected and separated by centrifugation (4000 rpm for 5 min) to remove the catalyst. The supernatant was filtered through a 0.22 μm membrane filter and then analyzed at wavelength of 350 nm by using a 752N UV-vis spectrophotometer.

2.4 Radical trapping experiments

At room temperature, 0.050 g of as-prepared samples and 1 mol benzoquinone (BQ) (or triethanolamine (TEOA), isopropyl alcohol (IPA)) were added to 50 mL of a 15 mg/L TC aqueous solution. And then the above mixed solution was magnetically stirred in the dark for 30 min to ensure the establishment of an adsorption-desorption equilibrium. After 500 W Xe lamp irradiation, approximately 5 mL of the sample solution at the given intervals were collected and separated by centrifugation (4000 rpm for 5 min) to remove the catalyst. The supernatant was filtered through a 0.22 μm membrane filter and then analyzed at wavelength of 350 nm by using a 752 N UV-vis spectrophotometer.

3. RESULTS AND DISCUSSION

The phase structure and purity of as-prepared samples were studied by XRD, and the diffractograms are shown in Fig.1. The result reveals that all the peaks of the sample were well matched with the Russellite Bi_2WO_6 (JCPDS 39-0256). No impurity peak was detected in the patterns, which suggests that the products of Bi_2WO_6 are identical crystalline phase.

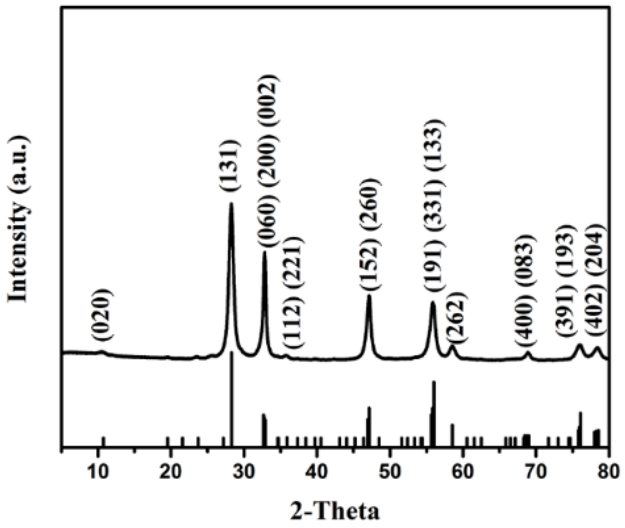

Figure 1. XRD diffractograms of the as-prepared samples

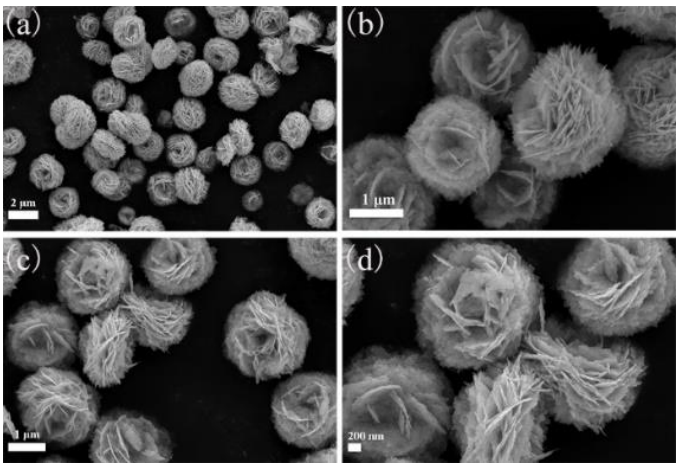

Figure 2. Low-magnified and high-magnified SEM images of the as-prepared samples

Panoramic images taken by SEM, as presented in Fig. 2a, directly display the Bi_2WO_6 products consisted of dispersive Bi_2WO_6 flower-like spheres. No other morphologies were observed in the as-prepared samples, which demonstrated the high yield growth of the flower-like spheres microstructures. Fig. 2b-d clearly shows that the Bi_2WO_6 flower-like spheres composed of numerous nanoplates. The TEM images of as-prepared samples (Figure 3a-c) presents an microspheres structure constructed with two-dimension nanosheets, in accordance with the SEM images (Fig. 2). The high-resolution TEM image displays that the lattice interplanar spacing was measured to be about 0.242 nm, which is corresponding to the spacing of (112) planes of Russellite Bi2WO6 (Figure 3d).

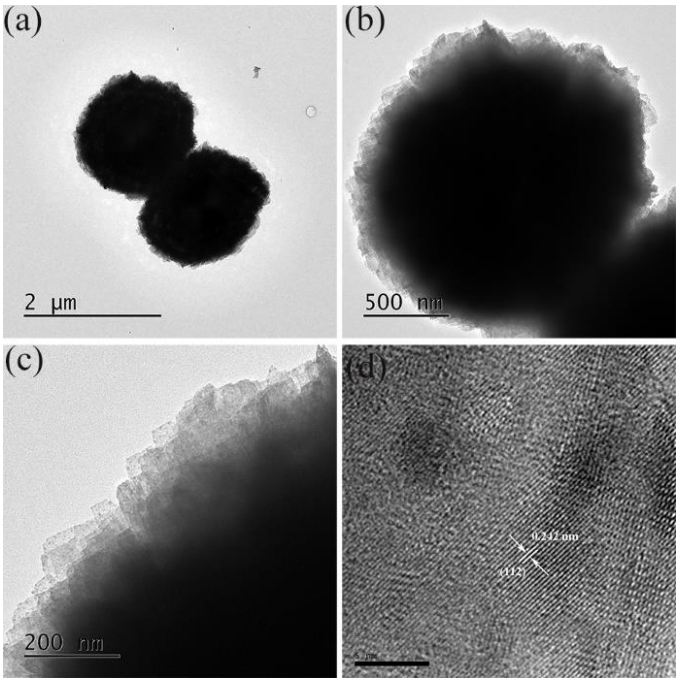

Figure 3. Low-magnified and high-magnified TEM images of the as-prepared samples

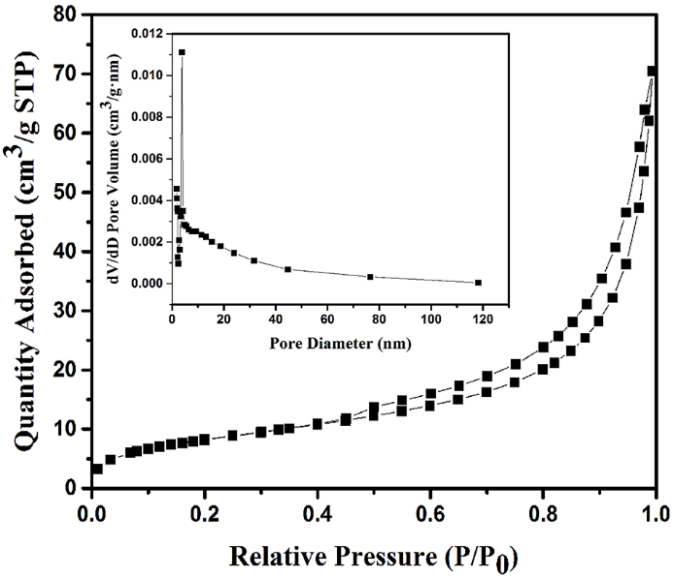

Figure 4. Nitrogen adsorption-desorption isotherms and the corresponding pore size distribution plot (inset) of Bi_2WO_6 flower-like spheres

The nitrogen adsorption-desorption isotherms and porosity of the Bi_2WO_6 flower-like spheres were further explored. The N_2 adsorption-desorption isotherms and the pore size distribution (inset) of Bi_2WO_6 flower-like spheres are presented in Fig. 4. The nitrogen adsorption and desorption isotherms were assigned as type IV, which is the characteristic isotherm of mesoporous materials [9-10]. As can be seen in Fig. 4 (inset), the data of pore-size distribution obtained from the isotherms shows the pore size range of Bi_2WO_6 flower-like spheres was 0-120 nm. Meamwhile, the surface area of the Bi_2WO_6 flower-like spheres was 30.22 m^2/g.

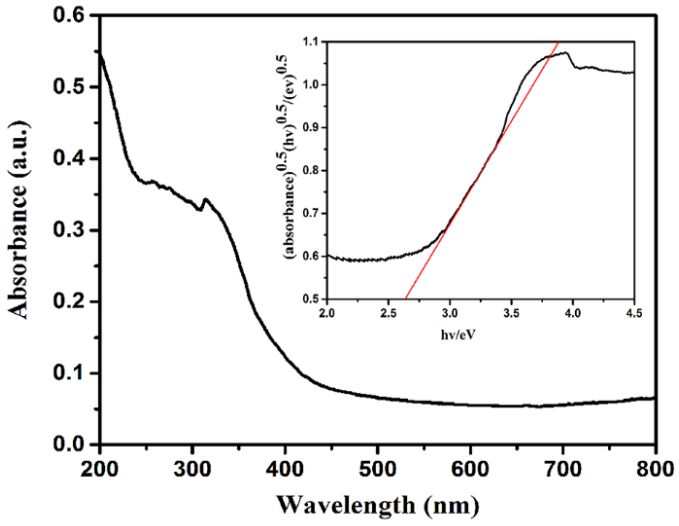

Figure 5. UV-vis DRS and $(Ah\nu)^{1/2}$-hν curves (insert) of the Bi_2WO_6 flower-like spheres

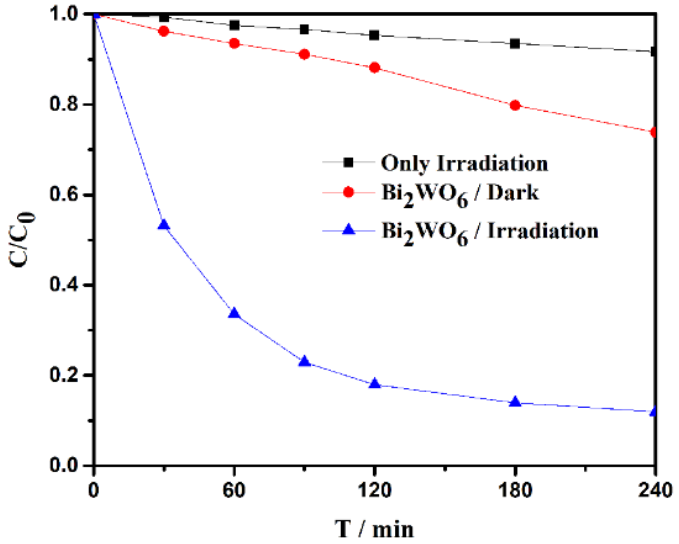

Figure 6. The photodegradation efficiencies of TC as a function of irradiation time by the Bi_2WO_6 flower-like spheres under 500 W Xe lamp light irradiation

As everyone knows that the optical absorption behaviors of a semiconductor are affected by the electronic structure features, which are regarded as crucial factors in judging its photocatalytic performance [11-12]. It is obvious that Bi_2WO_6 flower-like spheres showed a steep absorption edge of about 450 nm, reflecting that the visible light absorption is related to the band-gap transition rather than the transition from an impurity levels [4,13]. Fig.5 shows the UV-visible diffuse reflectance spectrum of the Bi_2WO_6 flower-like spheres. As can be seen in Fig. 5, the band gaps (E_g) of the product were estimated at approximately 2.64 eV. The Bi_2WO_6 flower-like spheres possess a narrowed band gap compared with that of previous reported [14-16], which indicates that Bi_2WO_6 flower-like spheres could have outstanding photocatalytic activity for TC photodecomposition under visible light irradiation.

The photocatalytic activity of the Bi_2WO_6 flower-like spheres was evaluated by the degrading the TC under visible light irradiation. Fig. 6 shows the blank tests, which indicates that photo-induced self-sensitized photodegradation scarcely influenced the result of the experiment. The result of dark absorption experiment shows that the Bi_2WO_6 flower-like spheres owned a certain amount of absorption to TC, which was beneficial to the photodegradation of Bi_2WO_6 flower-like spheres. Based on the principles of photocatalytic reaction, the main steps in the process occured on the surface of a semiconductor photocatalyst, so the adsorption of TC on the photocatalyst surface definitely affected the photocatalytic reaction and generally high adsorption capacity of catalyst favors the photocatalytic reaction [17-18]. The Bi_2WO_6 flower-like spheres exhibited excellent photocatalytic activities, 88% of TC could be photodegraded under visible light irradiation, which is higher than that reported in many other literatures [19-22] (shown Table 1). Fig. S1 shows that the Bi_2WO_6 flower-like spheres displayed well photocatalytic activity to TC despite the fact that the photodegradation performance of the Bi_2WO_6 flower-like spheres decreased with the increasing initial concentration of TC. This result can be attributed to fact that the Bi_2WO_6 flower-like spheres own narrowed band-gap, mesoporous flower-like structure composed of numerous nanosheets, and suitable BET areas, which can offer more surface-active sites for the TC adsorption and degradation. Moreover, the Ultra performance liquid

chromatography -mass spectrum (UPLC-MS) was utilized to investigate the mediates of photocatalytic degradation TC. According to the result of UPLC-MS (Figure S1) and the relative published articles[23-25], the probable photocatalytic degradation pathway would be speculated, as shown in Fig.7.

Table 1. Comparisons of TC degradation by different photocatalysts

Names of photocatalyst	Degraded pollutant	Amount of catalysts (g/L)	Concentration of TC (mg/L)	Degradation rate (%)	References
Bi2WO6	TC	1	15	88	This work
3D-PDI	TC	0.5	20ppm	~80	[19]
RGO-Cu_2O/Bi_2O_3	TC	0.5	10	75	[20]
$Ag/Bi_{3.84}W_{0.16}O_{6.24}$	TC	1	10	70	[21]
Ag/Bi_3TaO_7	TC	-	10	85.42	[22]

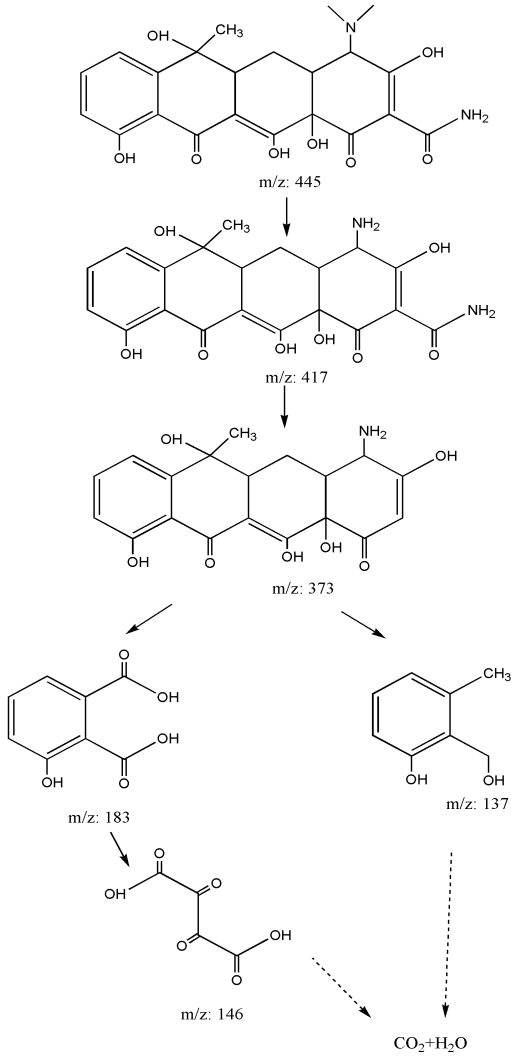

Figure 7. The probable photocatalytic degradation pathway of TC over Bi_2WO_6 flower-like spheres under 500 W Xe lamp light irradiation

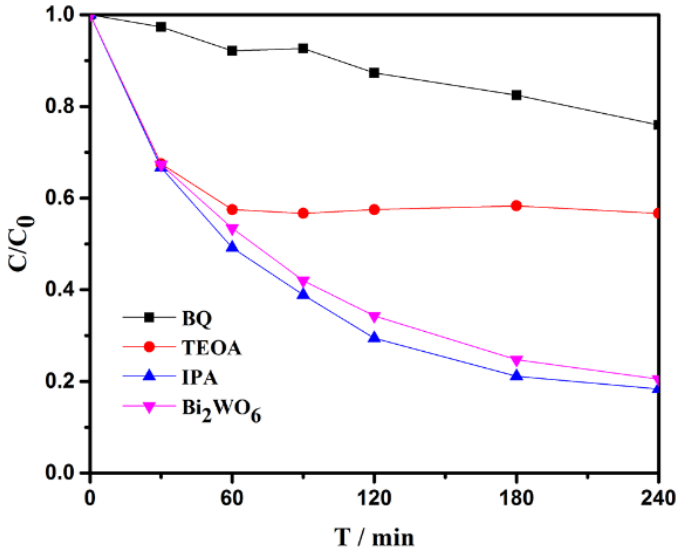

Figure 8. Photodegradation of TC over Bi_2WO_6 flower-like spheres in the presence of different scavengers under 500 W Xe lamp light irradiation

In order to investigate the photocatalytic mechanism of the Bi_2WO_6 flower-like spheres, we utilized the benzoquinone (BQ), triethanolamine (TEOA) and isopropyl alcohol (IPA) as a radical scavenger to trapping the superoxide ($O_2^{\bullet-}$), hole (h^+), hydroxyl free radical ($\bullet OH$) respectively. As shown in Fig.8, the degradation efficiency of TC showed a significant decrease when adding the BQ, which reveals that $O_2^{\bullet-}$ was main photogenerated activity species in the process of photodegradation TC. The degradation efficiency of TC was influenced by adding TEOA, showing that h^+ also contributed to the degradation of TC. On the contrary, the photocatalytic activity of the Bi_2WO_6 flower-like spheres was improved when adding IPA, which suggests the $\bullet OH$ was not main active species to the photodegradation TC. Hence, we can infer that superoxide radicals ($O_2^{\bullet-}$) and photogenerated holes (h^+) are the main active species for the photodegradation of TC over the Bi_2WO_6 flower-like spheres under visible light irradiation.

4. CONCLUSIONS

The Bi_2WO_6 flower-like spheres composed of nanosheets were successfully synthesized by hydrothermal reaction. The Bi_2WO_6 flower-like spheres possesses a strong absorption in the visible light region and have a narrowed bang gap, which can be good for the high photocatalytic activities under visible light irradiation. The study provides a general and effective method to the fabrication of Bi_2WO_6 flower-like spheres, which can have broader applications in the environmental treatment areas.

ACKNOWLEDGEMENTS
This work was supported by the Scientific Research Projects for High-Level Talents of Chongqing Technology and Business University (1956032), youth project of science and technology research program of Chongqing Education Commission of China (KJQN202000824, KJQN202000835).

SUPPLEMENTARY FIGURE

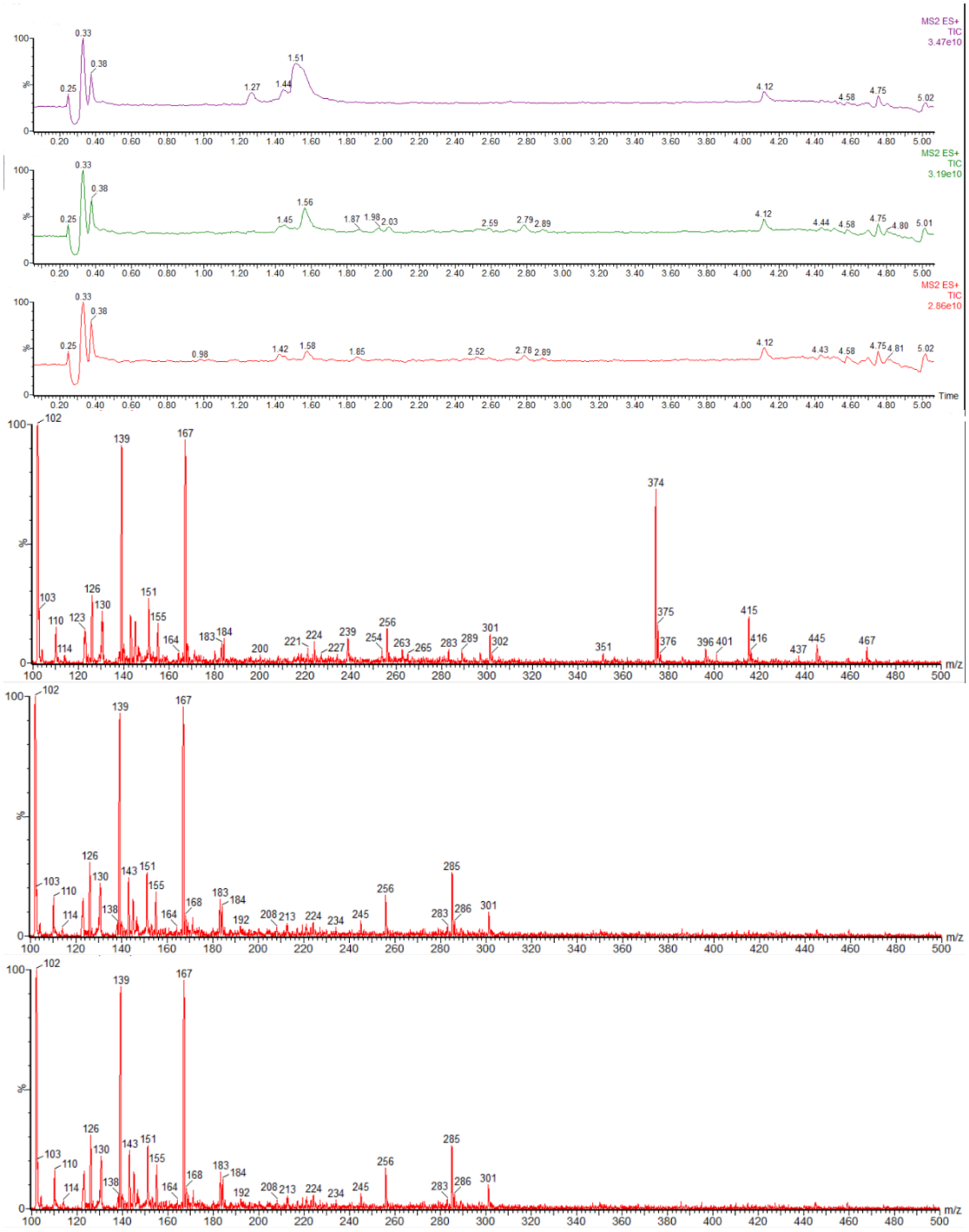

Figure S1. Ultra performance liquid chromatography mass spectrometry (UPLC-MS) images of the mesoporous Bi_2WO_6 flower-like spheres photodegradation TC under 500 W Xe lamp irradiation.

References

1. J.J. Wang, L.Tang, G.M. Zeng, Y.N. Liu, Y.Y. Zhou, Y.C. Deng, J.J. Wang and B. Peng, *ACS Sustainable Chem. Eng.,* 5 (2017) 1062.
2. N. Zhang, R. Ciriminna and M. Pagliaro, *Y.J. Chem. Soc. Rev.,* 43 (2014) 5276.

3. X.Y. Kong, W.L. Tan, B.J. Ng, S.P. Chai and A.R. Mohamed, *Nano Res.,* 10 (2017) 1720.
4. Y.Y. Li, J.P. Liu, X.T. Huang and G.Y. Li, *Cryst. Growth Des.,* 7 (2007) 1350.
5. S.J. Liu, Y.F. Hou, S.L. Zheng, Y. Zhang and Y. Wang, *Crystengcomm,* 15 (2013) 4124.
6. T. Saison, N. Chemin, C. Chaneac, O. Durupthy, V. Ruaux, L. Mariey, F. Mauge, P. Beaunier and J.P. Jolivet, *J. Phys. Chem. C,* 115 (2011) 5657.
7. H.L. Lv, X.H. Liang, G.B. Ji, H.Q. Zhang and Y.W. Du, *ACS Appl. Mater. Interfaces,* 7 (2015) 9776.
8. J.W. Bai, Y. Li, P. Jin, J.f. Wang and L. Liu, *J. Alloys Compd.,* 30 (2017) 809.
9. J.W. Bai, Y. Li, J.D Liu and L. Liu, *Microporous Mesoporous Mater.*, 240 (2017) 91.
10. H.B. Fu, S.C. Zhang, T.G. Xu, Y.F. Zhu and J.M. Chen, *Environ. Sci. Technol.,* 42 (2008) 2005.
11. C.Y. Wang, H. Zhang, F. Li and L.Y. Zhu, *Environ. Sci. Technol.,* 44 (2010) 6843.
12. J.W. Bai, Y. Li, P.K. Wei, J.D. Liu, W. Chen and L. Liu, *Small,* 15 (2019) e1900020.
13. L. Wang, W.Z Wang, M. Shang, W.Z. Yin, S.M. Sun and L. Zhang, *Int. J. Hydrogen Energy,* 35 (2009) 19.
14. L.S. Zhang, W.Z. Wang, Z.G. Chen, L. Zhou, H.L. Xu and W. Zhu, *J. Mater. Chem., 17* (2007) 2526.
15. Y.M. Liu, Z.W. Ding, H. Lv, J. Guang, S. Li and J.H. Jiang, *Mater. Lett.,* 157 (2015) 158.
16. X.F. Cao, L. Zhang, X.T. Chen and Z.L. Xue, *Crystengcomm,* 13 (2011) 306.
17. E. Grabowska, J. Reszczynska and A. Zaleska, *Water Res.,* 46 (2012) 5453.
18. M.S.F.A. Zamri and N. Sapawe, *Mater. Today. Proc.*, 19 (2019) 1261.
19. Q.C. Zhang, L. Jiang, J. Wang, Y.F. Zhu, Y.J. Pu and W.D. Dai, *Appl. Catal., B*, 277 (2020) 119122.
20. H.Q Shen, J.X Wang, J.H Jiang, B.F Luo, B.D Mao and W.D Shi, *Chem. Eng. J.,* 331 (2018) 242.
21. X.Y. Li, L.P. Wang, D.B. Xu, Ji.C. Lin, P. Li, S. Lin and W. D Shi, *CrystEngComm,* 17 (2015) 2421.
22. B.F. Luo, D.B. Xu, D. Li, G.L. Wu, M.M. Wu, W.D. Shi, and M. Chen, *ACS Appl. Mater. Interfaces,* 7(2015) 17061.
23. Q.C. Zhang, L. Jiang, J. Wang, Y.F. Zhu, Y.J. Pu and W.D. Dai, *Appl. Catal., B,* 277 (2020) 119122.
24. Y. Yang, Z.T. Zeng, C. Zhang, D.L. Huang, G.M. Zeng, R. Xiao, C. Lai, C.Y. Zhou, H. Guo, W.J. Xue, M. Cheng, W.J. Wang and J.J. Wang, *Chem. Eng. J.,* 349 (2018) 808.
25. N. Barhoumi, H. Olvera-Vargas , N. Oturan, D. Huguenot, A. Gadri, S. Ammar, E. Brillas and M. A. Oturan, *Appl. Catal., B,* 209 (2017) 637.